Water Air Soil Pollut (2014) 225:1817
DOI 10.1007/s11270-013-1817-5

Effects of Emissions from an Aluminium Smelter in a Tree Tropical Species Sensitive to Fluoride

Bruno Francisco Sant'Anna-Santos · Aristéa Alves Azevedo · Thiago Gonçalves Alves · Naiara Viana Campos · Marco Antônio Oliva · Vânia Maria Moreira Valente

Received: 24 February 2013 / Accepted: 14 November 2013 / Published online: 6 December 2013

Abstract Fluoride is among the most phytotoxic atmospheric pollutants, commonly linked to the appearance of lesions in susceptible plants around emitting sources. In order to assess the effects of fluoride on leaves of *Spondias dulcis* Parkinson (Anacardiaceae), plants were examined 78 km (non-polluted area) and 0.78 km (polluted area) from an aluminium smelter. The level of fluoride increased with the exposure time of the plants in the polluted area. On the third day of exposure in the polluted area, necroses with typical colouration were observed. Micromorphological damage began at the abaxial epidermis, mainly associated with the stomata. Starch grain accumulation was more pronounced in the midrib. The cell membranes and chloroplasts were greatly affected by the pollutant. We observed accumulation of phenolic compounds and electron-dense material at the boundaries of the ending veinlets. The microscopic events described precede the appearance of symptoms and are therefore of prognostic value in predicting injury by fluoride and will be useful as biomarkers. The high sensitivity of *S. dulcis* to fluoride and the specificity of the symptoms confirm, for the first time, in an experiment of active biomonitoring, the potential of this species as a bioindicator.

Keywords *Spondias dulcis* · Leaf anatomy · Active biomonitoring · Bioindicator

Abbreviations

E1	Experiment one
E2	Experiment two
DM	Dry matter
DE	Day of exposure

1 Introduction

The air quality monitoring of highly phytotoxic airborne fluoride in the vicinity of emitters is currently limited to sporadic investigations despite the growing importance of these activities in industrial countries and emerging economies (Franzaring et al. 2007). Fluoride is among the most phytotoxic atmospheric pollutants, commonly linked to the appearance of lesions in susceptible plants around emitting sources, especially factories that produce phosphate fertilisers, aluminium, glass, and ceramics (Weinstein and Davison 2004).

When the concentration of fluoride surpasses the natural level in the atmosphere, susceptible species present chlorotic and necrotic lesions on their leaves, a response determined by genetic and edaphoclimatic factors (Weinstein and Davison 2004). While low

B. F. Sant'Anna-Santos (✉) · A. A. Azevedo · T. G. Alves · N. V. Campos · M. A. Oliva · V. M. M. Valente
Departamento de Biologia Vegetal, Universidade Federal de Viçosa, Av. PH Rolfs, s/n, Centro, Viçosa 36570-000 Minas Gerais, Brazil
e-mail: brunoufv@yahoo.com.br

B. F. Sant'Anna-Santos
Universidade Federal de Minas Gerais, Campus Regional Montes Claros, Av. Universitária, 1000, Caixa Postal 135, Bairro Universitário, Montes Claros 39404-547 Minas Gerais, Brazil

concentrations of the pollutant may not cause the appearance of symptoms, they still may cause invisible damage to very sensitive species (Fornasiero 2003), so, studies of these plants on a microscopic level are warranted. The integrative evaluation of microscopic injury symptoms (leading to macroscopic symptoms) for their potential to diagnose the causative agent still awaits exploration because the macroscopic and microscopic levels have most often been studied independently of one another (Günthardt-Goerg and Vollenweider 2007). In studies of ozone, microscopic analysis has been used as a tool in validating the cause of stress (Vollenweider et al. 2003) and in detecting injuries in asymptomatic leaves (Reig-Arminaña et al. 2004).

The use of susceptible species has been proved a proper, low-cost methodology for detecting the effects of atmospheric pollutants on organisms (Klumpp et al. 2001). However, the following prerequisites must be considered when deciding what species to use: adaptation to the weather conditions of the target region; the potential to develop visible symptoms in the leaves (Strehl and Arndt 1989); and specific morpho-anatomical, physiological, and/or biochemical responses caused by the pollutant (Oliva and Figueiredo 2005). *Spondias dulcis* Parkinson (cajá-mirim), a perennial species from Polynesia and distributed across almost all of Brazil (Souza et al. 1998), develops typical fluoride-induced leaf symptoms like those identified in microscopic studies of plants exposed under laboratory conditions (Sant'Anna-Santos et al. 2012). However, the results obtained from the studies under controlled conditions must be carefully extrapolated to field conditions due to the artificial conditions of the experiments (Reig-Arminaña et al. 2004). Thus, it is essential to expose species with bioindicative potential to the emissions of a polluting source in the field and to compare the data obtained with results from the laboratory before concluding that the morphological changes and microscopic damage possess diagnostic value and can be used as biomarkers, respectively.

Assis et al. (2003) observed, in 2000 and 2002, concentrations of fluoride with maximum values between 6.22 and 12.87 μg m^{-3} at one monitoring station close to an aluminium smelter that has been working since the 1940s in Ouro Preto, Minas Gerais State, Brazil. According to the World Health Organization (WHO, 2002), the level of atmospheric inorganic fluoride is usually low (<0.05 μg m^{-3}) in non-polluted sites. Brazilian environmental legislation does not recognise any air quality standards for fluoride (Assis et al. 2003). Nevertheless, the relevant air quality limits adopted by several countries to protect sensitive plants are between 0.3 and 0.5 μg m^{-3} of HF (EU 2001; MOE 2005). Aluminium smelters can also be responsible for the emission of excessive concentrations of sulphur dioxide (SO_2). In Ouro Preto, SO_2 annual geometric mean showed values of 22 μg m^{-3} (Assis et al. 2003) that are acceptable considering the critical level of 20 μg m^{-3} SO_2 (annual mean) established in Europe for forest trees (Sanders et al. 1995). In industrial processes, the production of aluminium results in the formation of residues that must be disposed of in the environment after proper and safe treatment. In fact, technological advances have been diminishing emissions of this nature, but fluoride is still released in small amounts and may cause damage (Fornasiero 2003).

The vegetation around the aluminium smelter in Ouro Preto presents clear signs of fluoride contamination, including high levels of the pollutant in the leaves of widely dispersed herbaceous species in that region (Divan Junior et al. 2008). Despite the efforts of the company to diminish its industrial emissions, the fluoride content found in native species in proximity to the factory reached levels greater than 1,000 μg g^{-1} (Divan Junior et al. 2008), which according to Treshow and Anderson (1989) happens near sources that do not control their fluoride emissions.

The goals of this work were to assess the effects of fluoride emissions of an aluminium smelter on *S. dulcis* plants, to examine the potential use in the field of macroscopic and microscopic symptoms previously identified in controlled conditions (Sant'Anna-Santos et al. 2012) in diagnosis of injury and as biomarkers, respectively, and to identify ultra-structural damage caused by the pollutant.

2 Materials and Methods

2.1 Species and Culture Conditions

Plants of *S. dulcis* Parkinson (Anacardiaceae) were obtained from seminiferous propagation from a unique adult individual located at an altitude of 280 m, at the coordinates Lat 19°57′04″ S and Long 42°50′27″ W, mapped through the global positioning system (GPSII plus, Garmin Ltd., Hampshire, UK) at the boundaries of Nursery of Parque Estadual do Rio Doce-MG. Voucher specimen was stored at Herbarium VIC (Universidade Federal de Viçosa) under the number 29607.

Two months after sowing, the plants were transferred to a greenhouse for acclimation. The greenhouse was located at an altitude of 649 m, at the coordinates Lat 20°45′20″ S and Long 42°52′40″ W. After being transferred to 2.6-dm^3 pots, the plants received Hoagland 0.25-strength nutritive solution (Hoagland and Arnon 1950) every 5 days during the acclimation period (2 months) and until the end of the experiment, following the methodology proposed by Silva et al. (2000).

2.2 Location of Experiment

The plants were exposed to pollutant emissions from an isolated source of atmospheric fluoride emission from an aluminium smelter in Ouro Preto, Minas Gerais State, Brazil, according to the methodology adopted by Divan Junior et al. (2007)—0.78 km from a fluoride emission source located at an altitude of 1,101 m at the geographic coordinates Lat 20°24′09.7″ S and Long 43°31′14.8″ W. Another experimental station, called the "reference station," was installed at the Federal University of Viçosa, Minas Gerais State, Brazil, at an altitude of 649 m and at the geographic coordinates Lat 20°45′20″ S and Long 42°52′40″ W.

The plants were exposed in the field for one of two periods, designated experiments 1 and 2 (E1 and E2, respectively). In E1, from 3rd July 2006 until 12th July 2006, the samplings were scheduled to be done every 3 days. However, the plants began to show symptoms before the first sampling. Thus, in E2 (from 24th July 2006 to 27th July 2006), the samplings were done daily. All the plants were arranged in shelves placed 1.5 m from the ground as recommended by Divan Junior et al. (2007). The experiment was completely randomised with five repetitions in E1 and three repetitions in E2.

2.3 Evaluation of Fluoride Content and Morphological and Microscopical Damages

In the two periods of exposure of plants in the field, there was daily monitoring of the evolution of the symptoms. With regards to the analysis of the percentage of necrosed leaf area and quantification of fluoride in the dry matter (DM), samplings were performed on the third, sixth, and ninth day during E1 and daily during E2.

To evaluate necrosed leaf area, all leaves of each of the individual *S. dulcis* plants were digitalized and submitted for image analysis using Image Pro-Plus, version 4.1 for Windows® (Media Cybernetics, Silver Spring, MD, USA), to calculate the percentage of necrosed leaf area.

All leaves of each plant were dried in a stove at 70 °C and reduced to particles with dimensions of less than 1 mm using a Wiley grinder. Then, 0.5-g aliquots of each sample were extracted in 0.1-M perchloric acid (Garcia-Ciudad et al. 1985) using an ionic strength adjustment buffer (Larsen and Widdowson 1971) for potentiometric determination of total fluoride content. The analyses were carried out in duplicate and repeated twice.

For the classification of plants by their susceptibility to fluoride, we took into consideration the necrosed leaf area in relation to the fluoride content in leaf DM, adopting the following scale proposed by Klumpp et al. (1995): very susceptible (plants that present leaf symptoms with accumulation of fluoride less than 50 μg g^{-1} DM) and susceptible (plants that present leaf symptoms with accumulation of fluoride between 50 and 200 μg g^{-1} DM).

Concerning the microscopic analyses, the leaf samples were collected on the third, sixth, and ninth day during E1 and on the third day of exposure during E2. The fragments were taken out from the middle portion of the folioles under expansion from leaves located at the third or fourth knot (from the apical bud). In order to identify fluoride-injured prognostic microscopic characteristics, all the samples were collected from asymptomatic areas from the folioles with necrosis (in plants exposed to pollution). These samples were destined to the characterization of structural and ultra-structural damages, detection of phenolic compounds, starch, and micromorphological damages.

For the micromorphological analysis, samples fixed in Karnovsky's solution (Karnovsky 1965) were post-fixed in osmium tetroxide (1 %), dehydrated in ethylic series and dried to the critical point (equipment model CPD 020, Bal-Tec, Balzers, Liechtenstein). The leaflets were covered with gold using the cathodic spray process in a Sputter Coater (model FDU010, Bal-Tec, Balzers, Liechtenstein). Photographic documentation was performed using a scanning electron microscope with a digital camera (model Leo 1430 VP, Zeiss, Cambridge, England).

For the light microscopy, after fixation in Karnovsky's solution (Karnovsky 1965) and dehydration in ethylic series, the samples were placed in methacrylate (Historesin, Leica Instruments, Heidelberg, Alemanha). Transverse cuts (8 μm thick) were obtained in automatic rotary microtome (model RM2155, Leica Microsystems Inc., Deerfield, USA) and stained with Toluidine Blue,

pH=4.0 (O'Brien and McCully, 1981) for anatomical analysis. For the detection of starch, the cuts were submitted to lugol (Johansen 1940). The permanent slides were mounted with Permount.

Samples used for the histochemical test for detection of phenolic compounds were fixed in a solution of ferrous sulphate in formalin (Johansen 1940) for 24 h under vacuum, washed in distilled water, and submitted to dehydration in ethylic/butylic series. After embedding in histologic paraffin, the blocks were cut (10-μm thick) using a rotary microtome, and the slides were mounted in glycerine jelly (Kaiser 1880). For extraction of phenolic compounds (control), a portion of the samples was stored in methanol under vacuum for 72 h and then fixed according to the protocol described above for samples submitted to phenol detection. The images were obtained using a light microscope with a digital camera (model Olympus AX70TRF, Olympus Optical, Tokyo, Japan).

Regarding the ultra-structural analysis, after fixation in Karnovsky's solution (Karnovsky 1965), the samples were post-fixed in osmium tetroxide (1 %), dehydrated in crescent ethylic series, and embedded in Spurr resin (Spurr 1969). Transverse cuts, 70-nm thick, were performed with an ultramicrotome (model UCT, Leica Microsystems Inc., Deerfield, USA). The ultra-fine cuts were contrasted in uranyl acetate and lead citrate (Reynolds 1963) and recorded in transmission electron microscope (model Zeiss EM900) at 50 kV, coupled with a digital camera.

The data for fluoride content and percentage of necrosed leaf area were submitted to analysis of variance, using SAEG software (Euclydes 1983), and the means of the treatments were compared using Tukey's test at 5 % probability.

3 Results

With increasing time of exposure in both experiments E1 and E2, the levels of pollutant increased continuously in the plants located near the emitting source but remained constant at below 0.6 μg g^{-1} in the plants at the reference station. In E1, on the third day of exposure (DE), the level of fluoride accumulated in the leaves was almost eight times higher ($p<0.01$) than that observed at the reference station. In E2, the level of pollutant accumulated in the DM was approximately six times higher ($p<0.01$) after the first DE and 12 times higher after the third DE, compared to that observed in the reference station. Compared to the plants in E1, the plants exposed in E2 accumulated, in the same period of time (3 days of exposure), 67 % more fluoride in their leaves (Fig. 1a, b).

In E1, necroses appeared on the second DE, spread to 7.5 % of the total leaf area on the third DE and spread to approximately 60 % of the total leaf area at the end of the exposure (ninth DE) (Fig. 1c). In E2, necroses appeared earlier, right after the first DE, covering 4.5 % of the total leaf area. On the third DE, 14.5 % of total leaf area was already undergoing necrosis (Fig. 1d). Compared to the plants in E1, the plants in E2 presented 93 % more necroses on the third DE. The folioles of the plants exposed in the reference station became a bright green colour (Fig. 2a). As for those exposed in Ouro Preto, during both exposure periods, the necroses started from the margin, base, and apexes of the folioles (Fig. 2b–d). The lesions developed gradually, going through the lateral veins and midveins affecting some folioles completely. There were no chlorotic lesions observed in the leaves. The necroses had typical colouration: darkened, brown, and greyish (Fig. 2e, f).

Scanning electron microscopy revealed that the folioles of *S. dulcis* from the reference station had abaxial epidermis without trichomes but with stomata (Fig. 3a), and at the midrib region there were elongated epidermal cells and convex outer periclinal walls (Fig. 4a). In the adaxial epidermis, the epidermis presented conspicuous anticlinal wall contours and epicuticular waxes with a pulverulent character (Fig. 4c).

In the plants exposed in Ouro Preto in E1 and E2, damage was observed on the third DE, restricted to the abaxial epidermis and associated mainly with the stomata. In addition to ostioles obliterated by the fragments of the cuticle (Fig. 3b), we observed fungal hyphae close to or associated with the stomata (Fig. 3c); deformed stomatal outer ledges (Fig. 3d–f); concavities on the leaf surface (Fig. 3g); rupture of the epidermis and exposure of the internal tissues (Fig. 3h–j). However, in E2, the damage was more severe than in E1, with rupture of the epidermis on the third DE (Fig. 3k), an event observed only from the sixth DE onward in E1 (Fig. 3h). In E1, on the ninth DE, the epidermal cells of the midrib collapsed, forming grooves parallel to the longest axis of the leaf (Fig. 4b). On the adaxial epidermis, the damage started on the sixth DE, characterised by epicuticular waxes that were amorphous and/or eroded (Fig. 4d), less evident anticlinal wall contours and the presence of fungal hyphae (Fig. 4e), which formed a mass of fungal hyphae in some places (Fig. 4f).

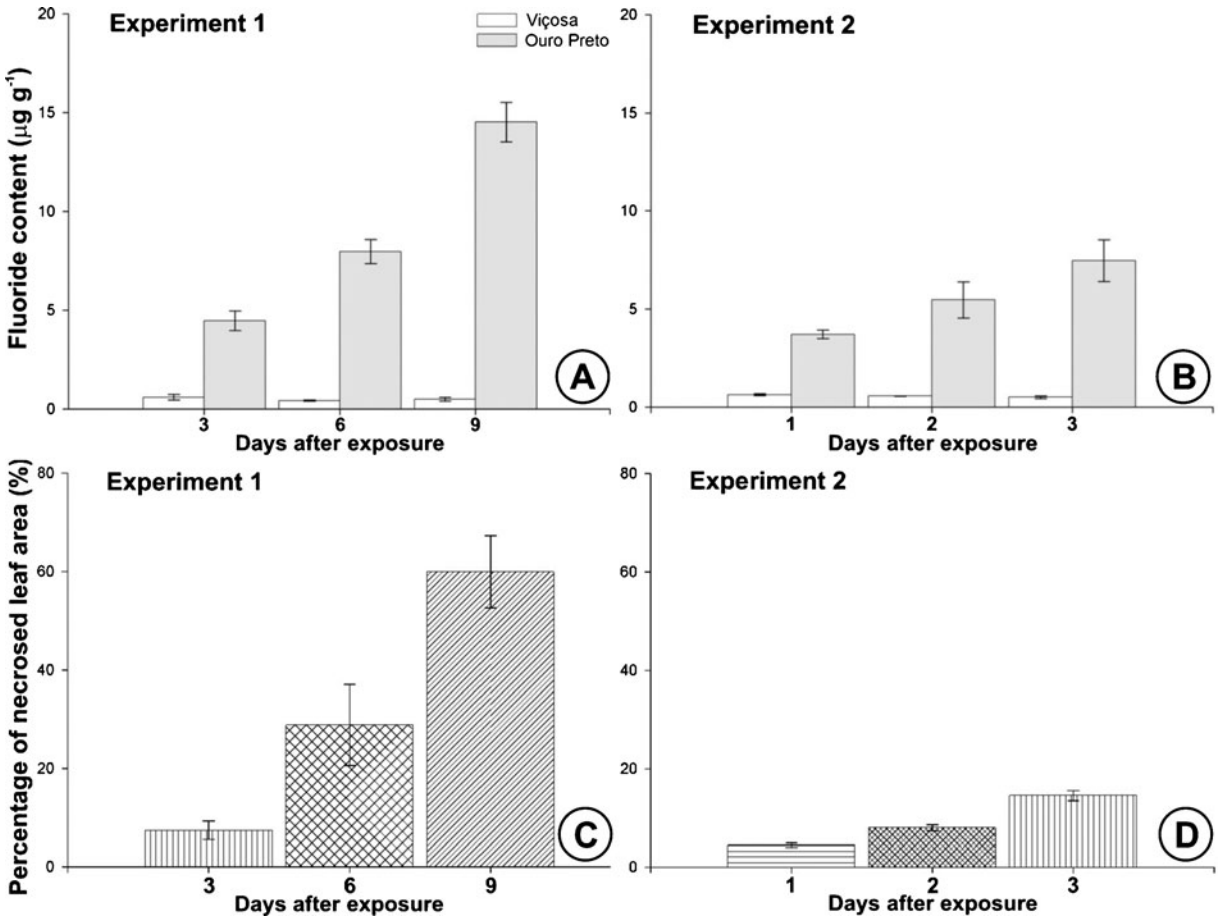

Fig. 1 Fluoride content (**a**–**b**) and percentage of necrosed area (**c**–**d**) in leaves of *S. dulcis* as a function of the time of exposure to a nearby fluoride emission source (Ouro Preto) and at the reference station (Viçosa): **a**, **c** experiment 1; **b**, **d** experiment 2. The *vertical bars* indicate the standard error

Light microscopy revealed that *S. dulcis* from the reference station had hypostomatic folioles with uniseriate epidermis and mesophyll formed by a layer of palisade parenchyma, four or five layers of spongy parenchyma (Fig. 5a), crystalliferous idioblasts containing druses (Figs. 5a, c; 6c) and vessel elements with helicoidal thickening of the secondary wall (Fig. 5e). The midrib showed collateral vascular bundles with a layer of fibres between the phloem and the cortical parenchyma (Fig. 5h). Testing with ferrous sulphate indicated the presence of idioblasts with phenolic compounds only in the midrib (Fig. 6a). Testing with Lugol showed the presence of starch in the midrib (Fig. 6b), as well as in the leaf mid-region (Fig. 6e).

The anatomical damage to the leaf blade of the plants exposed in Ouro Preto was clear on the third DE, in both E1 and E2, characterised by plasmolysis and retraction of the palisade parenchyma (Fig. 5b and d), as well as phenolic compound accumulation in the spongy parenchyma, at the adjacencies of the ending veinlets (Fig. 5f, g), and in the epidermis (Fig. 5i) and medullar parenchyma of the midrib (Fig. 6d). In the midrib, there was conspicuous starch grain accumulation in the cells of the medullar parenchyma (Fig. 6d), but in the leaf mid-region (Fig. 6f), starch grain accumulation was similar to that observed in *S. dulcis* from the reference station (Fig. 6e).

Transmission electron microscopy revealed that the samples collected from the reference station had organelles with peripheral disposition, chloroplasts with well-defined grana, starch grains with lobate shape, smooth cell wall, and vacuoles with hyaline content (Figs. 7a, 8a, c) and vessel elements with helicoidal thickening of the secondary wall (Fig. 8f).

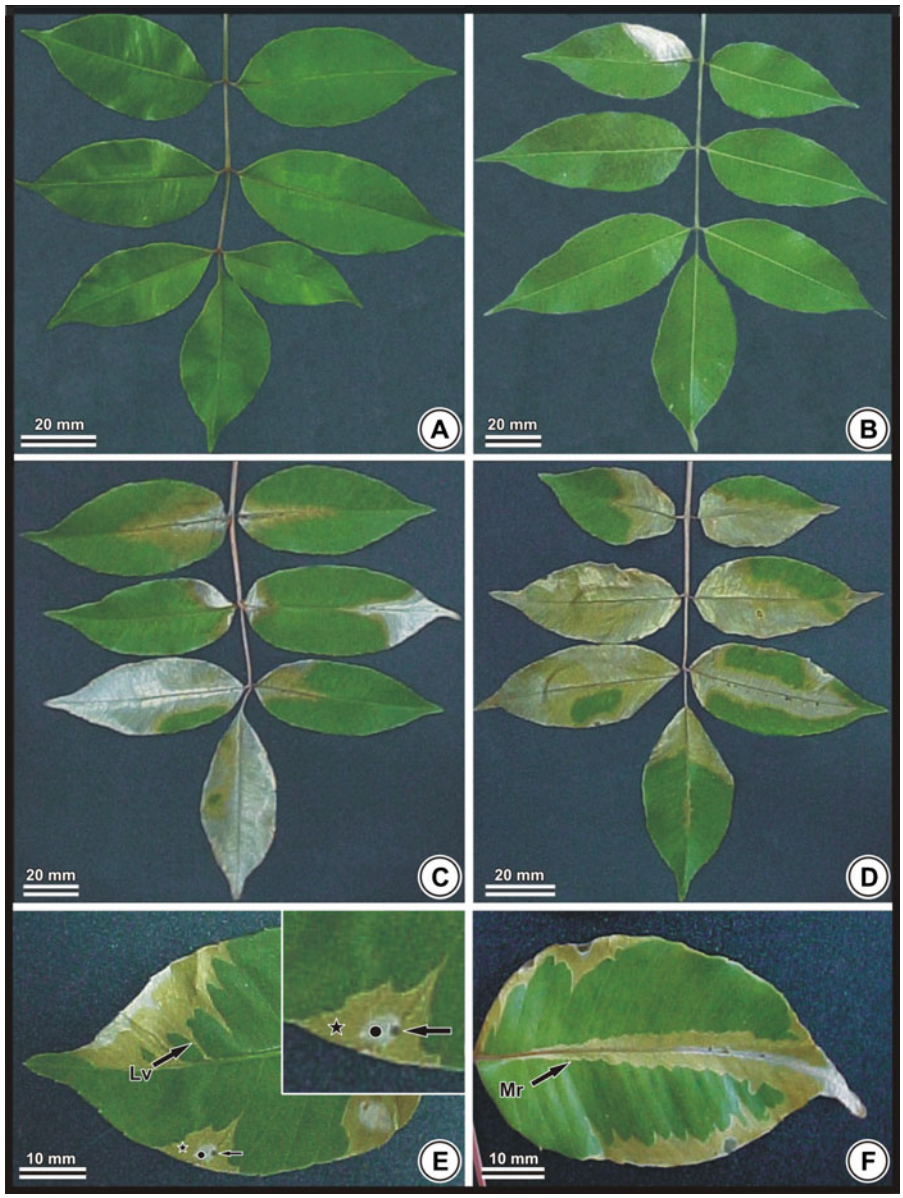

Fig. 2 Leaves of *S. dulcis* at the reference station (**a**) and on the third (**b**), sixth (**c**), and ninth (**d**–**f**) days of exposure to emissions of an aluminium smelter (experiment 1): **a** Bright green colouration; **b** Appearance of necrosis; **c** Necroses occurring in all folioles; **d** High percentage of necrosed leaf area; **e** Necrosis progressing through the lateral vein, consisting of three zones of distinct colourations: darkened (*arrow*), greyish (*circle*) and brown (*star*); (**f**) Necrosis progressing through the midrib. *Lv* lateral vein; *Mr* midrib

Ultra-structural damage to plants exposed in Ouro Preto started on the third DE in both E1 and E2. The cell walls acquired an undulate shape (Fig. 7b) showing re-entrances (Fig. 7c) and fibrillar aspects (Fig. 7e). The chloroplasts looked senescent (Fig. 7b, c); furthermore, there was an increase in the volume of the peripheral reticule (Fig. 7d), a disassembled lamellar system (Fig. 8d), and more voluminous starch grains (Fig. 8e) compared to the plants at the reference station. We observed an increase in the electron density and rupture of the cell membranes (Fig. 7d), and in some cells, the formation of concentric fragments (Fig. 8e). Besides the phenolic compound accumulation in the vacuoles of palisade (Fig. 7e) and spongy parenchyma cells (Fig. 8b), there was an increase in the

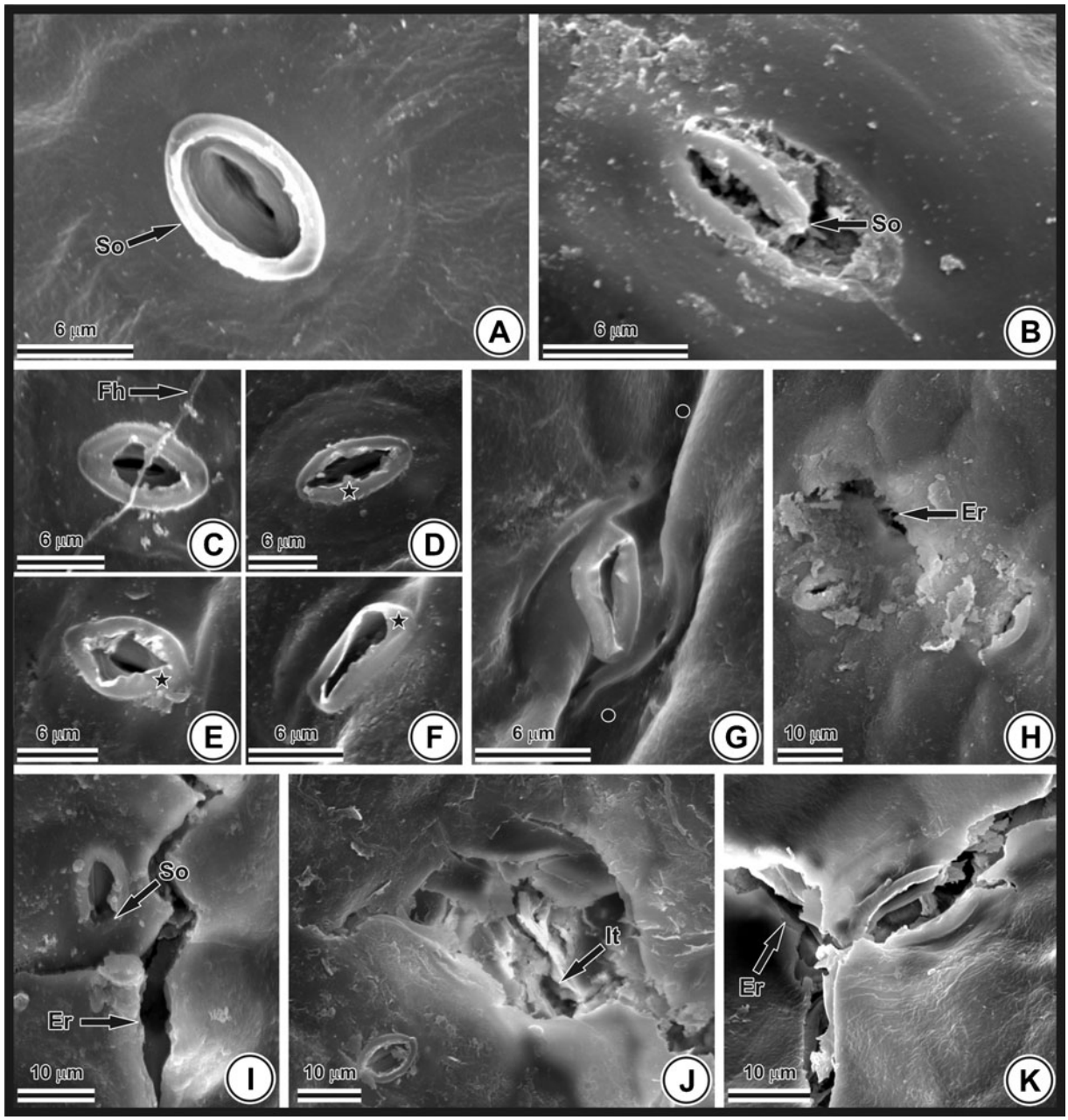

Fig. 3 Abaxial epidermis of the folioles of *S. dulcis* plants (scanning electron micrographs) not exposed to the pollution (**a**) and on the third (**b**, **k**), sixth (**c**–**h**), and ninth (**i**, **j**) days of exposure to emissions of the aluminium smelter in experiments 1 (**a**–**j**) and 2 (**k**): **a** Stomatal outer ledge; **b** Ostioles obliterated by cuticle fragments; **c** Fungal hyphae; **d**–**f** Deformed stomatal outer ledges (*stars*); **g** Concavities in the epidermis (*circles*); **h** Epidermis rupture; **i** Rupture of the stomatal outer ledge and the epidermis; **j** Exposure of the inner tissues; **k** Epidermis rupture in the adjacencies of the stomata. *So* stomatal outer ledge; *Er* epidermis rupture; *Fh* fungal hyphae; *It* inner tissue

amount of electron-dense rough material in the adjacencies and within the vessel elements, and there was a gradual increase of this material with increasing time of exposure (Fig. 8g, h).

4 Discussion

Fluoride accumulated quickly in the leaves of *S. dulcis* plants located 0.78 km from the fluoride source, as was

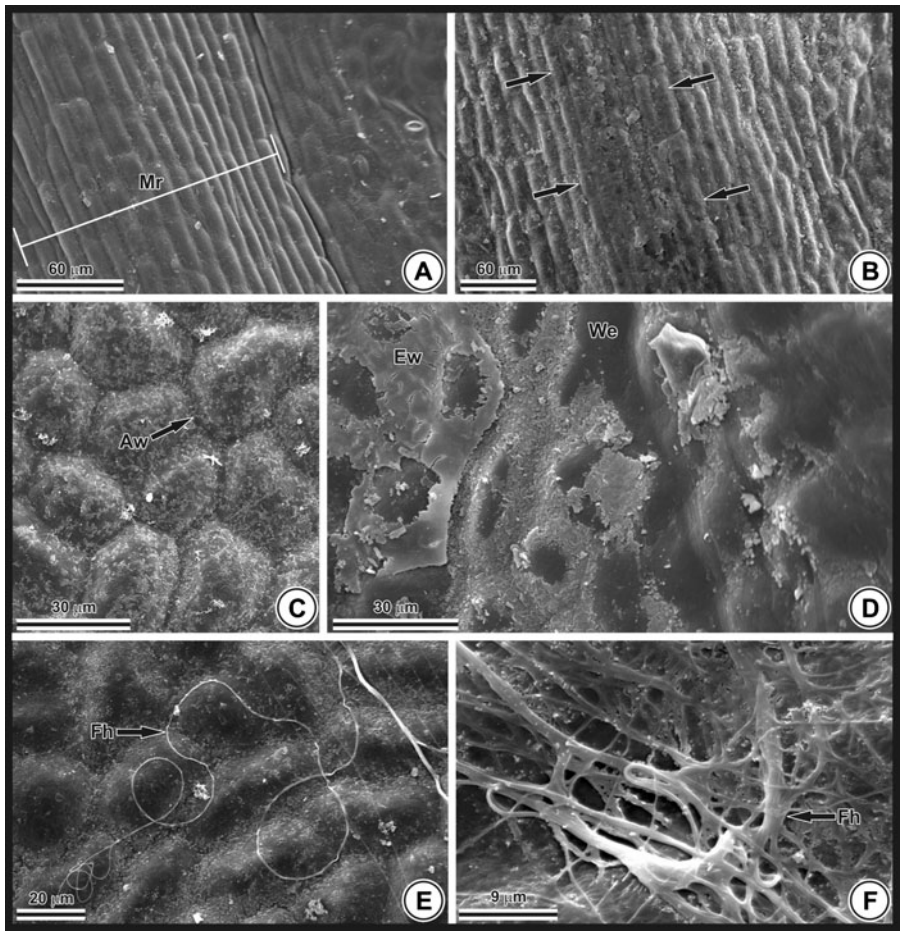

Fig. 4 Abaxial (**a**, **b**) and adaxial (**c**–**f**) epidermis of the folioles of the plants of *S. dulcis* (scanning electron micrographs) not exposed to the pollution (**a**, **c**) and on the sixth (**d**–**f**) and ninth (**b**) days of exposure to emissions of the aluminium smelter (experiment 1): **a** Midrib; **b** Grooves (*arrows*) in midrib; **c** Anticlinal walls well-defined and pulverulent epicuticular wax; **d** Erosion of epicuticular waxes and amorphous aspect; **e** Anticlinal walls with less evident contour and the presence of fungal hyphae; **f** Mass of fungal hyphae. *Mr* midrib; *Aw* anticlinal wall; *Ew* epicuticular wax; *We* wax erosion; *Fh* fungal hyphae

also observed in plants of *Chloris gayana* Kunth and *Panicum maximum* Jacq. exposed in the same area (Divan Junior et al. 2007). Heavy accumulation of pollutants in the leaves after a short period of exposure suggests that the plants were exposed to high levels of fluoride in the atmosphere (Fornasiero 2003).

In both experiments with *S. dulcis* performed in the winter, the fluoride content increased with the time of exposure of the plants in Ouro Preto but remained constant in the reference station, confirming the pollution by fluoride in proximity to the emitting source. Generally, the fluoride content in plants is determined by the concentration in the atmosphere, time of exposure, and species' absorption ability (Vike 1999). We observed greater accumulation of the pollutant in E2 than in E1 in *S. dulcis* exposed for the same duration of time (3 days), indicating that variation in the accumulation of the pollutant is related to differences in fluoride concentration in the atmosphere. Episodic variations in fluoride emission into the atmosphere are common events in areas near emitting sources (Divan Junior et al. 2008).

The greatest percentage of the symptoms observed 3 days after exposure of the plants in Ouro Preto in E2, in comparison to E1, is correlated with the highest concentration of the pollutant in the leaves. In *S. dulcis*, necroses occupied 29 % of the leaf area with levels of fluoride less than 8 μg g^{-1}, demonstrating a higher sensitivity of this species relative to *P. maximum* (Divan Junior et al. 2007) and justifying the classification of the

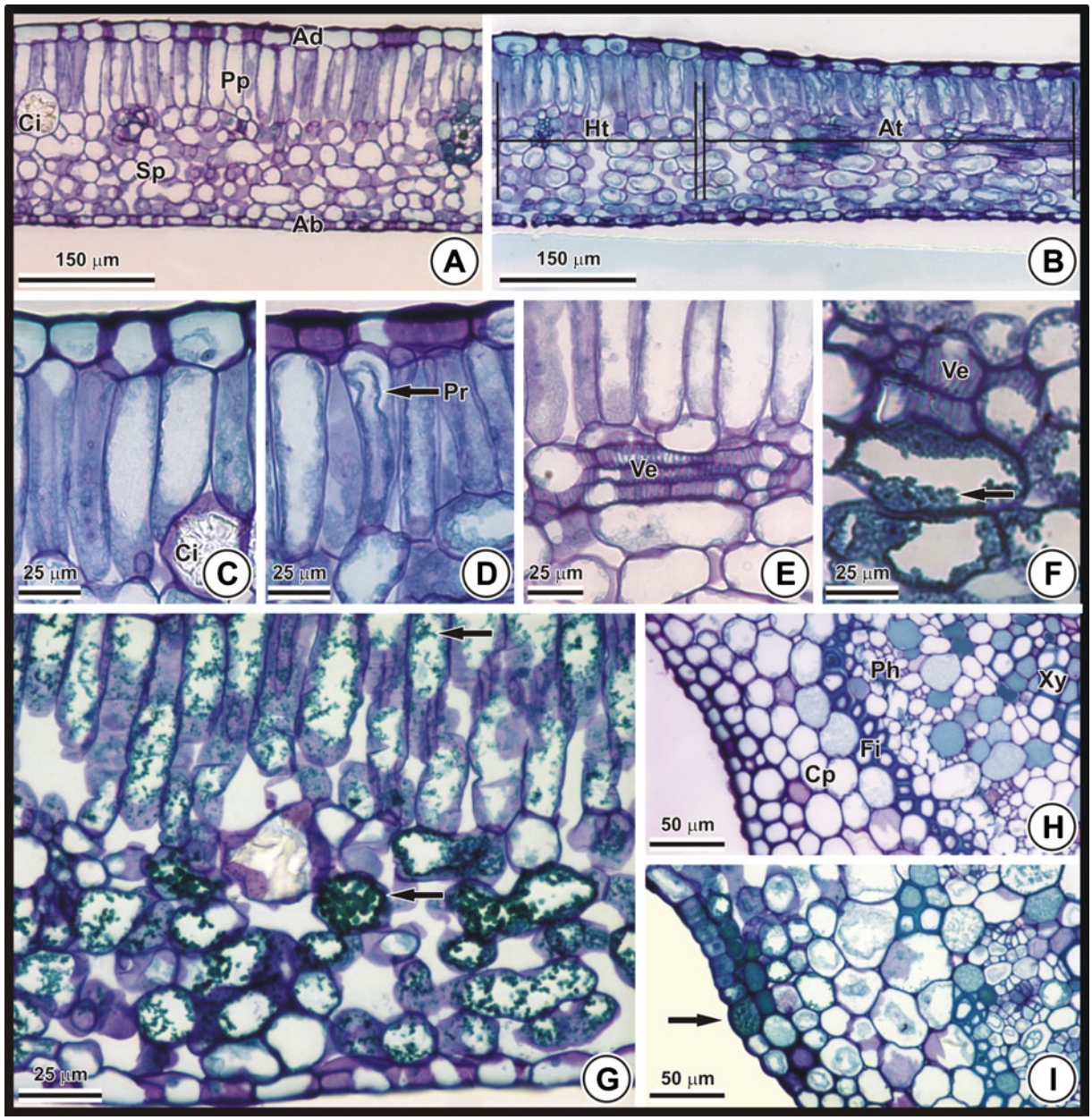

Fig. 5 Leaf blade structure of *S. dulcis* (light microscopy of transverse sections) not exposed to the pollution (**a**, **c**, **e**, **h**) and on the third (**b**, **d**), sixth (**f**), and ninth (**g**, **i**) days of exposure to emissions of the aluminium smelter (experiment 1): **a** Leaflet mid-region; **b** Plasmolysis of the palisade parenchyma; **c** Crystalliferous idioblast; **d** Protoplast retraction; **e** Vessel element; **f**, **g** Accumulation of phenolic compounds (*arrows*) in the adjacencies of the ending veinlets (**f**) and in parenchyma (**g**); **h** Midrib; **i** Accumulation of phenolic compounds (*arrow*) in the epidermis. *Ad* adaxial epidermis; *Ab* abaxial epidermis; *Ci* crystal idioblast; *Pp* palisade parenchyma; *Sp* Spongy parenchyma; *Ht* healthy tissue; *At* affected tissue; *Pr* protoplast retraction; *Ve* vessel element; *Cp* cortical parenchyma; *Fi* fibres; *Ph* phloem; *Xy* xylem

species as "very susceptible" according to the scale of Klumpp et al. (1995). When fluoride accumulates in the tissues and reaches lethal concentrations, it causes lesions in the leaves (Coulter et al., 1985), but susceptibility varies with the species (Weinstein and Davison 2004; Mezghani et al. 2005; Abdallah et al. 2006; Divan Junior et al. 2008; Mesquita et al. 2011). Leave of *Prunus armeniaca* L. exhibit necroses with

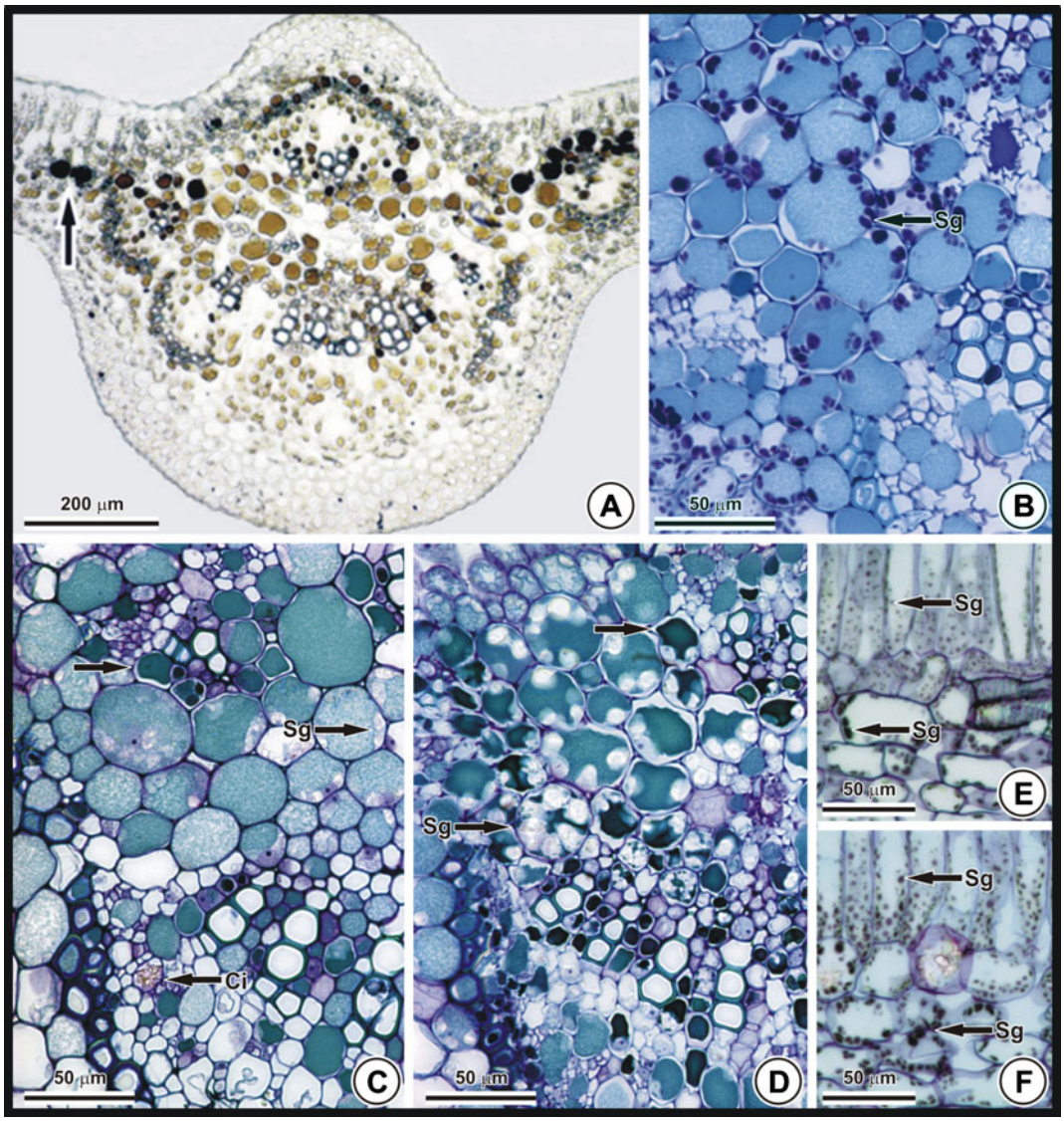

Fig. 6 Leaf blade structure of *S. dulcis* (light microscopy of transverse sections) not exposed to the pollution (**a**–**c**, **e**) and on the ninth (**d**, **f**) days of exposure to emissions of the aluminium smelter (experiment 1): **a** Midrib submitted to the test for detection of phenolic compounds: positive reaction in idioblasts (*arrow*); **b** Positive reaction to Lugol showing starch grains; **c** Peripheral starch grains and phenolic compounds in parenchyma (*arrow*); **d** Accumulation of starch grains and phenolic compounds (*arrow*); **e** Leaf mid-region; **f** Starch accumulation. *Sg* starch grain; *Ci* crystalliferous idioblast

65 μg g^{-1} of fluoride in the dry matter, while *Olea europaea* L. may accumulate up to 300 μg g^{-1} of fluoride in the dry matter of its leaves without exhibiting any symptoms of phytotoxicity to the pollutant (Mezghani et al. 2005). Variations in the amount accumulated and the tolerance to the element occur between species (Mezghani et al. 2005; Oliva and Figueiredo 2005; Divan Junior et al. 2008; Mesquita et al. 2011) and between cultivars (Fortes et al. 2003; Oliva and Figueiredo 2005).

The symptomatology observed in the present study was similar to that recorded in the laboratory (Sant'Anna-Santos et al. 2012), supporting the conclusion in biomonitoring that the cause of the stress in *S. dulcis* may be a consequence of abnormal amounts of fluoride in the leaves. In the field, the symptomatology has been used to monitor the effects of the stress caused by several biotic and abiotic factors (Vollenweider and Günthardt-Goerg 2006), including fluoride (Fornasiero 2003; Mezghani et al. 2005).

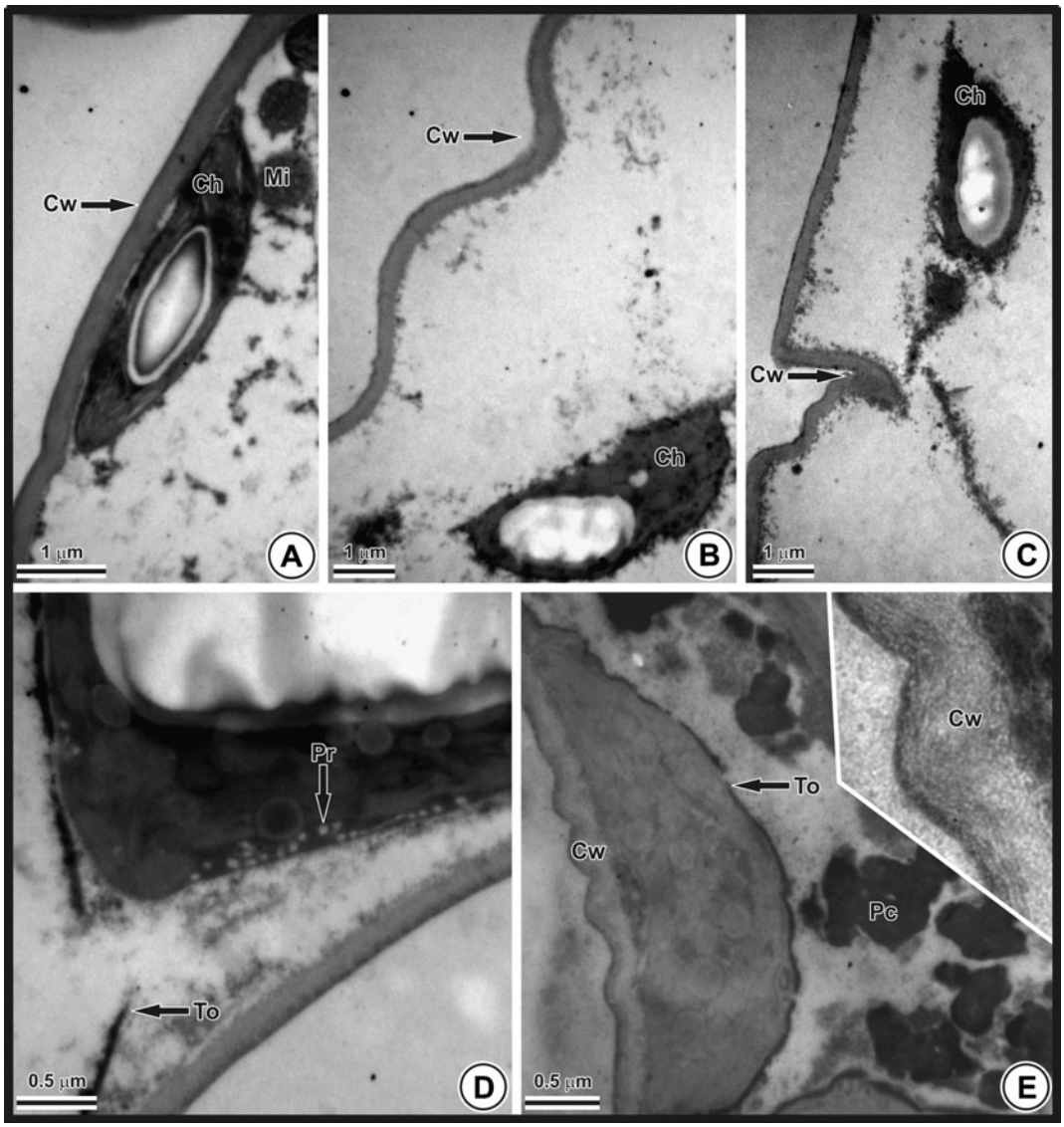

Fig. 7 Palisade parenchyma of *S. dulcis* (transmission electron microscopy of transverse sections) not exposed to the pollution (**a**) and on the third (**b**), sixth (**c**, **d**), and ninth (**e**) days of exposure to emissions of the aluminium smelter (experiment 1): **a** Smooth cell wall; **b** Undulate cell wall and chloroplast with senescent aspect; **c** Cell wall with re-entrances and senescent chloroplast; **d** Increase in the volume of the peripheral reticule and increase in electron density and rupture of tonoplast; **e** Cell wall with fibrillar aspect and phenolic compound accumulation in the vacuole. *Ch* chloroplast; *Cw* cell wall; *Mi* mitochondria; *To* tonoplast; *Pr* peripheral reticulum; *Pc* phenolic compound

Though there are detailed descriptions of the damage caused by fluoride, such as visible red areas on both surfaces of the leaf and "burn" of the leaf apex in *Hypericum perforatum* L. (Fornasiero 2003), the symptoms are generally described as apical and marginal chloroses and necroses, in the laboratory (Fornasiero 2001; Chaves et al. 2002) as well as in the field (Mezghani et al. 2005; Divan Junior et al. 2007; 2008). The lack of detail in the description of the symptoms limits the usefulness of the parameter for a more precise diagnosis in the field, which is needed to pinpoint the origin of the stress.

The detailed description of the symptoms are especially important for assess areas of industrial development where the plants are usually exposed to a combination of air pollutants. In the vicinity of aluminium

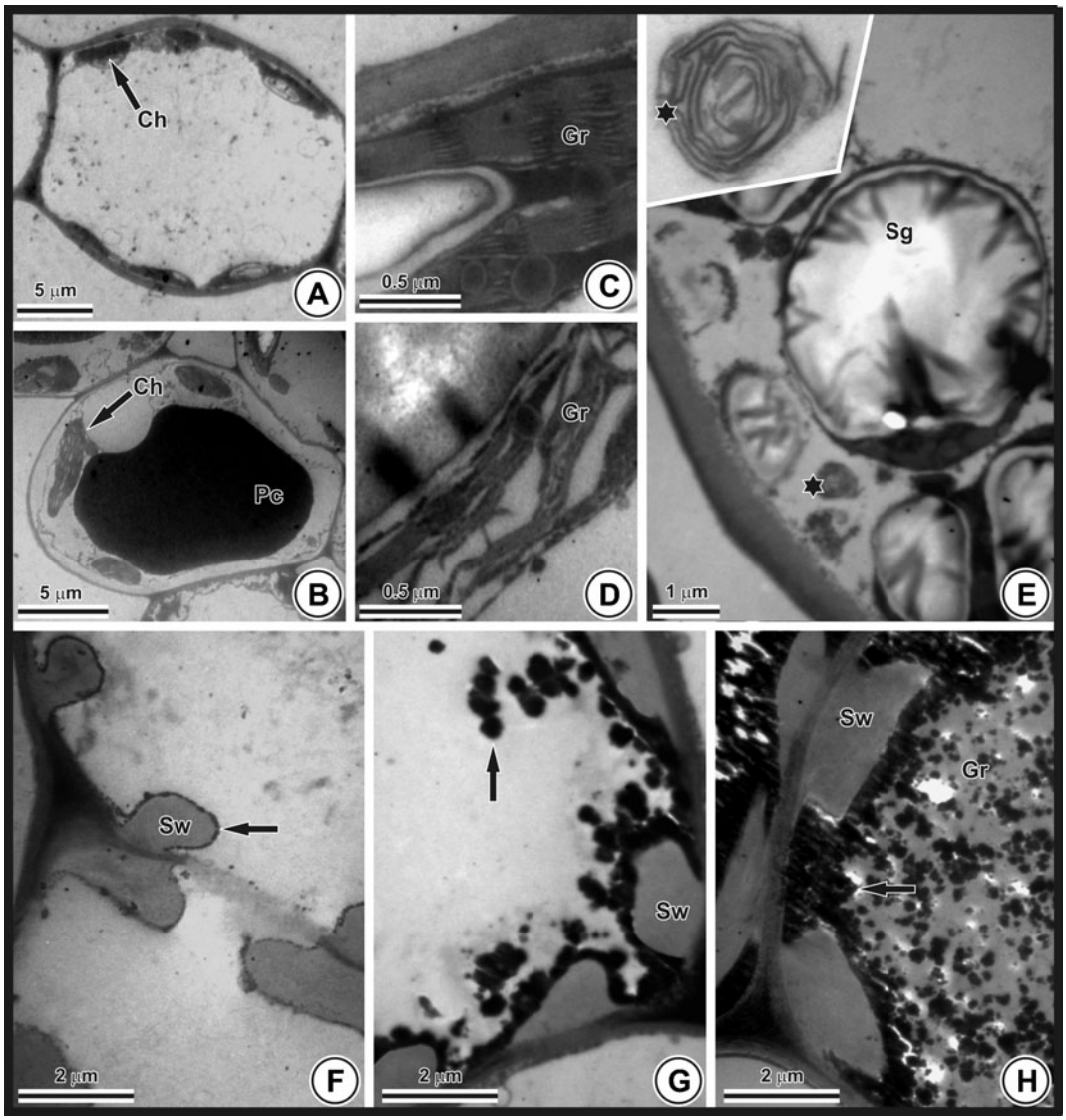

Fig. 8 Spongy parenchyma (**a**–**e**) and vessel elements (**f**–**h**) of *S. dulcis* (transmission electron microscopy of transverse sections) not exposed to the pollution (**a**, **c**, **f**) and on the third (**e**, **g**) and ninth (**b**, **d**, **h**) days of exposure to emissions of the aluminium smelter (experiment 1): **a** Vacuole with hyaline content; **b** Vacuole full of phenolic compounds; **c** Chloroplasts with well-defined grana; **d** Chloroplast showing a disassembled lamellar system; **e** Voluminous starch grains and concentric fragments of cell membranes (*star*) in detail; **f** Vessel elements with helicoidal thickening of the secondary wall; **g**–**h** Increase in the amount of electron-dense rough material (*arrow*) in the adjacencies and within the vessel elements. *Ch* chloroplast; *Gr* grana; *Pc* phenolic compound; *Sg* starch grain; *Sw* secondary wall

factors, other agents like sulphur dioxide (SO_2) can mimic fluoride-induced injury. However, the chlorotic or necrotic injury caused by SO_2 are known to be confined to the interveinal area of the leaf (Weinstein and Davison 2004), differing to the fluoride necrosis described in this work that develop along the veins and the foliar margin.

In a similar way to most atmospheric pollutants, gaseous fluoride penetrates the plants through the stomata, which are associated with most of the damage present in *S. dulcis* plants exposed in Ouro Preto. The initial appearance of damage beginning on the abaxial surface is related to restriction of the stomata to this leaf surface in this species (Silva et al. 2000).

The damage observed on the adaxial surface of the leaves of plants exposed in Ouro Preto is probably due to the potentialising effect of the dew, frequently observed during the period of the experiments (winter), which dissolves the pollutant resultant from the dry deposition, favouring the removal of the epicuticular waxes and loss of cuticle structure. The removal of these hydrophobic layers probably facilitates the establishment of the fungi observed on both surfaces of the leaves exposed to the factory's emissions, since surfaces that present a film of water promote colonisation by microorganisms (Barthlott 1981). Removal of the epicuticular waxes and infestation by fungal hyphae were reported in the laboratory (Sant'Anna-Santos et al. 2012), but these microorganisms were not detected in the control plants. These observations were also found to be true for the plants exposed in Ouro Preto, indicating that the pollution is responsible for promoting fungal infestation via removal of the epicuticular waxes.

Loss of turgidity of the epidermal cells in the plants exposed in Ouro Preto was the probable cause of the modification of the anticlinal wall outlines in both surfaces of the leaf. The plasmolysis of the epidermal cells was more intense in the abaxial surface of the leaf, where the stomata are the main entryway for the pollutant, and in the midrib. Despite being practically deprived of stomata, the prominent curvature formed by the midrib in the relief of the leaf may predispose this region to more time in contact with the pollutant dissolved in the dew. In plants of *Magnolia ovata* (A. St.-Hil.) Spreng. exposed to fluoride simulated rain, the epidermal cells suffer a gradual reduction of volume that is more intense near the necrosis (Sant'Anna-Santos et al. 2007).

Histochemical tests revealed the presence of phenolic compounds in the leaves of *S. dulcis*, as was observed in the stem of this species by Sant'Anna-Santos et al. (2006c). Dark contents intensely stained green by toluidine blue were observed in the midrib and in the adjacencies of the ending veinlets in the leaves of *S. dulcis* exposed in Ouro Preto. In general, phenolic compounds are stained green by toluidine blue (Briggs et al. 2005). Other authors, such as Fornasiero (2003) and Mesquita et al. (2012), have already suggested the possibility of phenol accumulation in plants exposed to fluoride; however, specific tests have not been performed to confirm this possibility. The accumulation of phenols has been interpreted as a mechanism of defence of the plants, activated by biotic and abiotic factors that induce stress in the plant (Vaughn and Duke 1984). The accumulation of electron-dense material inside the vessel elements probably reflects the transport of fluoride through the xylem. Additionally, macroscopic observations suggest that necrosis progression through the vascular tissues is more pronounced in the midrib, reinforcing the hypothesis that fluoride acts in the vascular system.

The ultra-structural changes in the plasma membrane observed in *S. dulcis* were similar to those seen in the mesophyll of *H. perforatum*, where the plasma membrane, frequently broken, appears detached from the cell wall (Fornasiero 2001). The results obtained by Rakowski et al. (1995) in *Pinus strobus* L. indicate that the plasma membrane may be one of the initial sites of the injuries caused by fluoride. Divan Junior et al. (2007) observed a significant effect of fluoride on membrane integrity by increasing the release of cell electrolytes in plants with high accumulation of pollutants. Fluoride modifies the lipid-protein interactions of the membranes, altering metabolic functions (Rakowski 1997), such as the activity of the enzyme H^+-ATPase (Façanha and de Meis 1995), increasing membrane permeability.

Among the organelles, chloroplasts showed a greater variety of ultra-structural alterations in the plants exposed in Ouro Preto. In the literature, the symptoms attributed to fluoride are normally the following: stromal swelling and thylakoid coiling; less distinct lamellar system; increase in the number and size of plastoglobules; accumulation of starch grains; in some cases, increase in the number, size, and electron density of the plastoglobules; rupture of the external cover and alteration in the shape of the chloroplasts (Wei and Miller 1972; Thomson 1975; Soikkeli and Tuovinen 1979; Soikkeli 1981; Zwiazek and Shay 1987; Eleftheriou and Tsekos 1991; Anttonen 1992; Holopainen et al. 1992; Miller 1993; Wulff and Kärenlampi 1996; Fornasiero 2001).

In *S. dulcis*, there was an increase in the volume of the starch grains of the chloroplasts. The occurrence of cells with an abnormal amount of starch has already been reported in *S. dulcis* under stress caused by acid rain (Sant'Anna-Santos et al. 2006a; 2006b) and is related to the inhibitory effect of the pollutant on the translocation of carbohydrate from the leaves to the roots, causing the accumulation of starch grains in the chloroplasts (Rennenberg et al. 1996). The accumulation of starch grains was also evidenced in the mesophyll of the leaves of *Pinus halepensis* Mill. exposed to urban pollution (Soda et al. 2000). These authors suggested that starch accumulation was a consequence of

the collapse and inactivation of the phloem. This phenomenon might be indicative of acceleration in the cell-ageing process under the influence of the pollutants (Schmitt and Ruetze 1990).

5 Conclusion

The high sensitivity of *S. dulcis* to fluoride, the specificity of the symptoms, and the high correlation between symptomatology and levels of fluoride all combine to confirm for the first time, in an experiment of active biomonitoring, the potential of *S. dulcis* as a bioindicator. Microscopic observations of the leaves collected in Ouro Preto were similar to observations in plants exposed to fluoride in the laboratory (Sant'Anna-Santos et al. 2012), which demonstrate that all the events described precede the appearance of macroscopic symptoms, thus guaranteeing that these parameters have prognostic value in predicting injury by fluoride and will be useful as biomarkers.

Acknowledgments The authors thank CAPES for a scholarship; the Nursery of Parque Estadual do Rio Doce-MG (NPERD) for supplying the plants; and the Laboratório de Anatomia Vegetal (Universidade Federal de Ouro Preto-UFOP), Núcleo de Microscopia e Microanálise (Universidade Federal de Viçosa-UFV) and Núcleo de Apoio à Pesquisa em Microscopia Eletrônica Aplicada à Pesquisa Agropecuária (Universidade de São Paulo-USP) for helping with the microscopy portion of this work.

References

Abdallah, F. B., Elloumi, N., Mezghani, O., Boukhris, M., & Garrec, J. (2006). Survival strategies of pomegranate and almond trees in a fluoride polluted area. *Comptes Rendus Biologies, 329*(3), 200–207.

Anttonen, S. (1992). Changes in lipids of Pinus sylvestris needles exposed to industrial air pollution. *Annales Botanici Fennici, 29*(2), 89–99.

Assis, C. M., Silveira, I. L., Anizelli, R. C. M. (2003). Automonitoramento da qualidade do ar em Ouro Preto/MG. In: Congresso Interamericano de Qualidade do Ar, 3., Canoas. Anais Porto Alegre, AIDIS, ABES, 2003. 1 CD-ROM

Barthlott, W. (1981). Epidermal and seed surface characters of plants: systematic applicability and some evolutionary aspects. *Nordic Journal of Botany, 1*(3), 345–355.

Briggs, C. L., Morris, E. C., & Ashford, A. E. (2005). Investigations into seed dormancy in *Grevillea linearifolia*, *G. buxifolia* and *G. Sericea*: anatomy and histochemistry of the seed coat. *Annals of Botany, 96*(6), 965–980.

Chaves, A. L. F., Silva, E. A. M., Azevedo, A. A., Cano, M. A. O., & Matsuoka, K. (2002). Ação do flúor dissolvido em chuva simulada sobre a estrutura foliar de Panicum maximum Jacq. (colonião) e Chloris gayana Kunth. (capim-Rhodes) – Poaceae. *Acta Botânica Brasílica, 16*(1), 395–406.

Coulter, C. T., Pack, M. R., & Sulzbach, C. W. (1985). An evaluation of the dose-response relationship of fluoride injury to gladiolus. *Atmospheric Environment, 19*(6), 1001–1007.

Divan Junior, A. M., Oliva, M. A., Martinez, C. A., & Cambraia, J. (2007). Effects of fluoride emissions on two tropical grasses: *Chloris gayana* and *Panicum maximum* cv. Colonião. *Ecotoxicology Environmental Safety, 67*(2), 247–253.

Divan Junior, A. M., Oliva, M. A., & Ferreira, F. A. (2008). Dispersal pattern of airborne emissions from an aluminium smelter in Ouro Preto, Brazil, as expressed by foliar fluoride accumulation in eight plant species. *Ecological Indicators, 8*(5), 454–461.

Eleftheriou, E. P., & Tsekos, I. (1991). Fluoride effects on leaf cell ultrastructure of olive trees growing in the vicinity of aluminium factory of Greece. *Trees, 5*(1), 83–98.

EU (2001). *European Union Risk Assessment Report: Hydrogen Fluoride*, CAS-No.: 7664-39-3. 1st Priority List, vol. 8, 134 pp

Euclydes, R. F. (1983). *Sistema de Análises Estatísticas e Genéticas da UFV (SAEG) – Manual*. Viçosa, Minas Gerais: CPD/UFV, Divisão de Pesquisas e Desenvolvimento, 74p

Façanha, A. R., & de Meis, L. (1995). Inhibition of maize root H+-ATPase by fluoride and fluoroaluminate complexes. *Plant Physiology, 108*(1), 241–246.

Fornasiero, R. B. (2001). Phytotoxic effects of fluorides. *Plant Science, 161*(5), 979–985.

Fornasiero, R. B. (2003). Fluorides effects on Hypericum perforatum plants: first field observations. *Plant Science, 165*(3), 507–513.

Fortes, C., Duarte, A. P., Matsuoka, S., Hoffmann, H. P., & Lavorenti, N. A. (2003). Toxicidade de flúor em cultivares de milho em área próxima a uma indústria de cerâmica, Araras (SP). *Bragantia, 62*(2), 275–281.

Franzaring, J., Klumpp, A., & Fangmeier, A. (2007). Active biomonitoring of airborne fluoride near an HF producing factory using standardised grass cultures. *Atmospheric Environment, 41*(23), 4828–4840.

Garcia-Ciudad, A., Garcia-Criado, B., & Pontón-San Emeterio, C. (1985). Determination of fluoride in plant samples by a potentiometric method and near-infrared reflectance spectroscopy. *Communications in Soil Science and Plant Analysis, 16*(10), 1107–1122.

Günthardt-Goerg, M. S., & Vollenweider, P. (2007). Linking stress with macroscopic and microscopic leaf response in trees: new diagnostic perspectives. *Environmental Pollution, 147*(3), 467–488.

Hoagland, D. R., & Arnon, D. I. (1950). *The water-culture method for growing plants without soil*. Berkeley, CA: California Agricultural Experiment Station.

Holopainen, T. H., Anttonen, S., Wulff, A., Palomäki, V., & Kärenlampi, L. (1992). Comparative evaluation of effects of gaseous pollutants, acid deposition and mineral deficiencies: structural changes in cells of forest plants. *Agriculture, Ecosystems & Environment, 42*(3–4), 341–398.

Johansen, D. A. (1940). *Plant microtechnique* (p. 523). New York: McGraw Hill.

Kaiser, E. (1880). Verfahren zur Herstellung einer tadellosen glycerin-gelatine. *Botanische Centralbl, 180*, 25–26.

Karnovsky, M. J. (1965). A formaldehyde-glutaraldehyde fixative of high osmolarity for use in electron microscopy. *Journal of Cell Biology, 27*(1), 137A–138A.

Klumpp, G., Klumpp, A., Domingos, M., & Guderian, R. (1995). Hemerocallis as bioindicator of fluoride pollution in tropical countries. *Environmental Monitoring and Assessment, 35*(1), 27–42.

Klumpp, A., Ansel, W., Klumpp, G., & Fomin, A. (2001). Um novo conceito de monitoramento e comunicação ambiental: a rede européia para avaliação da qualidade do ar usando plantas bioindicadoras (EuroBionet). *Brazilian Journal of Botany, 24*(4), 511–518.

Larsen, S., & Widdowson, A. E. (1971). Soil fluorine. *Journal of Soil Science, 22*(2), 210–221.

Mesquita, G. L., Tanaka, F. A. O., Cantarella, H., & Mattos, D. (2011). Atmospheric absorption of fluoride by cultivated species. Leaf structural changes and plant growth. *Water, Air & Soil Pollution, 219*(1–4), 143–156.

Mezghani, I., Elloumi, N., Abdallah, F. B., Chaieb, M., & Boukhris, M. (2005). Fluoride accumulation by vegetation in the vicinity of a phosphate fertilizer plant in Tunisia. *Fluoride, 38*(1), 69–75.

Miller, G. W. (1993). The effect of fluoride on higher plants. *Fluoride, 26*(1), 3–22.

MOE (2005). *Ontario Air Standards For Hydrogen Fluoride. Standards Development Branch Ontario Ministry of the Environment*, 112 pp

O'Brien, P. P., & McCully, M. E. (1981). *The study of plants structure principles and selected methods* (p. 45p). Melbourne, Australia: Termarcarphi Pty. Ltda.

Oliva, M. A., & Figueiredo, J. G. (2005). Gramíneas bioindicadoras da presença de flúor em regiões tropicais. *Brazilian Journal of Botany, 28*(2), 389–397.

Rakowski, K. J. (1997). Hydrogen fluoride effects on plasma membrane composition and ATPase activity in needles of white pine (*Pinus strobus*) seedlings pretreated with 12 h photoperiod. *Tree, 11*(4), 248–253.

Rakowski, K. J., Zwiazek, J. J., & Sumner, M. J. (1995). Hydrogen fluoride effects on plasma membrane composition, ATPase activity and cell structure in needles of eastern white pine (*Pinus strobus*) seedlings. *Tree, 9*(4), 190–194.

Reig-Arminaña, J., Calatayud, V., Cerveró, J., García-Breijo, F. J., Ibars, A., & Sanz, M. J. (2004). Effects of ozone on the foliar histology of the mastic plant (*Pistacia lentiscus* L.). *Environmental Pollution, 132*(2), 321–331.

Rennenberg, H., Herschbach, C., & Polle, A. (1996). Consequences of air pollution on shoot–root interactions. *Journal of Plant Physiology, 148*(3–4), 296–301.

Reynolds, E. S. (1963). The use of lead citrate at high pH as an eletron-opaque stain in electronmicroscopy. *Journal of Cell Biology, 17*(1), 208–212.

Sanders, G.E., Skärby, L., Ashmore, M.R., & Fuhrer, J. (1995). Establishing critical levels for the effects of air pollution on vegetation. *Water, Air and Soil Pollution, 85*(1), 189–200.

Sant'Anna-Santos, B. F., Silva, L. C., Azevedo, A. A., & Aguiar, R. (2006a). Effects of simulated acid rain on leaf anatomy and micromorphology of *Genipa americana* L. (Rubiaceae). *Brazilian Archives of Biology and Technology, 49*(2), 313–321.

Sant'Anna-Santos, B. F., Silva, L. C., Azevedo, A. A., Araújo, J. M., Alves, E. F., Silva, E. A. M., et al. (2006b). Effects of simulated acid rain on the foliar micromorphology and anatomy of tree tropical species. *Environmental and Experimental Botany, 58*(1–3), 158–168.

Sant'Anna-Santos, B. F., Thadeo, M., Meira, R. M. S. A., & Ascensão, L. (2006c). Anatomia e histoquímica das estruturas secretoras do caule de Spondias dulcis Forst. F. (Anacardiaceae). *Revista Árvore, 30*(3), 481–489.

Sant'Anna-Santos, B. F., Duque-Brasil, R., Azevedo, A. A., Silveira, A. S., Araújo, J. M., & Aguiar, R. (2007). Utilização de parâmetros morfoanatômicos na análise da fitotoxidez do flúor em folhas de Magnolia ovata (A. St.-Hil.) Spreng. (Magnoliaceae). *Revista Árvore, 31*(4), 761–771.

Sant'Anna-Santos, B. F., Azevedo, A. A., Silva, L. C., & Oliva, M. A. (2012). Diagnostic and prognostic characteristics of phytotoxicity caused by fluoride on *Spondias dulcis* Forst. F. (Anacardiaceae). *Anais da Academia Brasileira de Ciências, 84*(3), 689–702.

Schmitt, U., & Ruetze, M. (1990). Structural changes in spruce and fir needles. *Environmental Pollution, 68*(3–4), 345–348.

Silva, L. C., Azevedo, A. A., Silva, E. A. M., & Oliva, M. A. (2000). Flúor em chuva simulada: sintomatologia e efeitos sobre a estrutura foliar e o crescimento de plantas arbóreas. *Brazilian Journal of Botany, 23*(1), 385–393.

Soda, C., Bussotti, F., Grossoni, P., Barnes, J., Mori, B., & Tani, C. (2000). Impacts of urban levels of ozone on *Pinus halepensis* foliage. *Environmental and Experimental Botany, 44*(2000), 69–82.

Soikkeli, S. (1981). Comparison of cytological injuries in conifer needles from several polluted industrial environments in Finland. *Annales Botanici Fennici, 18*(1–4), 47–61.

Soikkeli, S., & Tuovinen, T. (1979). Damage in mesophyll ultrastructure of needles of Norway spruce in two industrial environments in central Finland. *Annales Botanici Fennici, 16*(1–4), 50–64.

Souza, F. X., Sousa, F. H. L., & Melo, F. I. O. (1998). Aspectos morfológicos de endocarpos de cajarana (Spondias cytherea sonn. - Anacardiaceae). *Revista Brasileira de Sementes, 20*(2), 141–146.

Spurr, A. R. (1969). A low-viscosity epoxy resin embedding medium for electron microscopy. *Journal of Ultrastructure Research, 26*(1–2), 31–43.

Strehl, T., & Arndt, U. (1989). Alterações apresentadas por Tillandsia aeranthos e T. recurvata (Bromeliaceae) expostas ao HF e SO_2. *Iheringia, 39*(1), 3–17.

Thomson, W. W. (1975). Effects of air pollutants on plant ultrastructure. In J. B. Mudd & T. T. Kozlowski (Eds.), *Responses of plants to air pollution* (pp. 179–194). New York: Academic.

Treshow, M., & Anderson, F. K. (1989). *Plant stress from air pollution* (p. 283pp). Chichester: John Wiley.

Vaughn, K., & Duke, S. O. (1984). Function of polyphenol oxidase in higher plants. *Physiologia Plantarum, 60*(1), 106–112.

Vike, E. (1999). Air-pollutant dispersal patterns and vegetation damage in the vicinity of three aluminium smelters in Norway. *Science of the Total Environment, 236*(1–3), 75–90.

Vollenweider, P., Günthardt-Goerg, M. S. (2006). Erratum to "Diagnosis of abiotic and biotic stress factors using the

visible symptoms in foliage" [Environ. Pollut. 137 (2005) 455–465]. *Environmental Pollution*, 140(3), 562–571

Vollenweider, P., Ottiger, M., & Günthardt-Goerg, M. S. (2003). Validation of leaf ozone symptoms in natural vegetation using microscopical methods. *Environmental Pollution, 124*(1), 101–118.

Wei, L., & Miller, G. W. (1972). Effect of HF on the fine structure of mesophyll cells from *Glycine max* Merr. *Fluoride, 5*(2), 67–73.

Weinstein, L. H., & Davison, A. W. (2004). *Fluorides in the environment* (p. 287). Effects on plants and animals. Wallingford: CABI Publishing.

WHO, World Health Organization (2002). *Fluoride. Environmental Health Criteria* 227

Wulff, A., & Kärenlampi, L. (1996). Effects of long-term open-air exposure to fluoride, nitrogen compounds and SO_2 on visible symptoms, pollutant accumulation and ultrastructure of Scots pine and Norway spruce seedlings. *Trees, 10*(3), 157–171.

Zwiazek, J. J., & Shay, J. M. (1987). Fluoride- and drought-induced structural alterations of mesophyll and guard cells in cotyledons of jack pine (*Pinus banksiana*). *Canadian Journal of Botany, 65*(11), 2310–2317.